Macromolecular Rapid Communication

www.mrc-journal.de

Chlorinated Polymers for Efficient Solar Cells with High Open Circuit Voltage: The Influence of Different Thiazole Numbers

Xiyue Yuan, Qian Wang, Dangqiang Zhu, Bilal Shahid, and Renqiang Yang**

The chlorination strategy has gradually become a promising approach to improve the open circuit voltage (V_{OC}) in polymer solar cells. In this work, by using an efficient thiazole-induced strategy in a polymer backbone, three thieno[3,4-*b*]thiophene (TT)-based polymers—PBClTTz-0, PBClTTz-1, and PBClTTz-2—are designed and synthesized with a Cl-substituted benzodithiophene (BDT) moiety and a thiazole unit as a π spacer. As expected, all of the polymers show a desirable open circuit voltage (V_{OC}) of >0.94 V in the solar cells; specifically, the voltage can reach 1.01 V for polymer PBClTTz-2 with two thiazole moieties. In addition, due to the excellent surface morphology and weak recombination of the active layer, photovoltaic devices based on PBClTTz-1 with one thiazole unit exhibit the highest power conversion efficiency (PCE) of 8.42%, which is noticeably superior to the fluorinated analogue PBClTTz-0 (6.85%). This work reveals the influence of the thiazole unit in a quinoid polymer backbone and confirms that the Donor-Acceptor(π)-Quinoid strategy is a promising construction method in molecular design.

Polymer solar cells (PSCs) have been intensively investigated due to their advantages of being lightweight, flexible, low-cost, and transparent large-area devices.[1–6] In the past, the power conversion efficiency (PCE) has been pushed to over 14% by means of new material designs and device engineering.[7,8] Moreover, obtaining favorable frontier orbital energy levels containing the highest occupied molecular orbital (HOMO) and lowest unoccupied molecular orbital (LUMO) is one of the key factors in realizing broad optical absorption and desirable open circuit voltage (V_{OC}) in the photovoltaic devices,[9–11] and the solar cells with high V_{OC} could be more desirable under low light intensity for practical applications.

To address the above issue, for many donor–acceptor (D–A) systems, the introduction of a heteroatom could be one effective approach to lower HOMO energy levels, including in fluorine, chlorine, and sulfur atoms.[12–16] However, the drawbacks of a relatively low yield from the fluorination reaction and the strong reducibility of sulfur atoms restrict their application.[7,17–21] In contrast, the chlorination strategy has attracted intense attention due to its short synthetic route, easy purification, and high yield.[22] For example, He et al. reported on the polymer PBTCl, based on the chlorinated quinoid acceptor thieno[3,4-*b*]thiophene(TT), which exhibited a noticeably decreased HOMO level, thereby leading to a high V_{OC} of 0.91 V in photovoltaic devices.[19] In addition, Hou et al. introduced a chlorine atom into the side chain of the donor benzodithiophene (BDT) unit, and further constructed polymer PBDB-T-2Cl, which also exhibited a sharp decrease in the HOMO energy level and excellent miscibility with the electron acceptor.[7] Conversely, polymer backbone modification could also efficiently modulate the energy levels. Yang et al. previously introduced a weak acceptor thiazole unit as a π bridge into the main backbone of the quinoid polymer and developed a new Donor-Acceptor(π)-Quinoid strategy. With the introduction of a thiazole (Tz) moiety, the HOMO energy level significantly decreased, and the backbone planarity increased. Accordingly, the V_{OC} gradually increased from 0.68 V for polymer PBDTTT-E-T without thiazole to 0.78 V for polymer PBTzT-4 with one thiazole unit and 0.83 V for polymer PTBTz-2 with two units.[23–25] In addition, the position of the halogen atom also has a significant impact on intermolecular self-assembly of the conjugated polymers.[26,27] Thus, by combining the aforementioned efficient chlorination strategy that is performed on the side chains with the thiazole-induced method that is performed on the polymer backbone, highly efficient photovoltaic materials with low HOMO energy levels could be expected with a desirable V_{OC} in corresponding devices.

In this work, three TT-based polymers, PBClTTz-0, PBClTTz-1, and PBClTTz-2, were designed and synthesized (**Figure 1**) with a Cl-substituted BDT moiety as the donor building block to study the influence of the introduction of a chlorine atom and different thiazole numbers. As expected, all chlorinated polymers showed the low HOMO energy level of <−5.5 eV. In this instance, the Tz unit in the backbone also acted exactly as an F atom on the side chain; meanwhile, with the increase in the thiazole unit number, the HOMO energy level decreased further. When fabricated into photovoltaic

X. Yuan, Q. Wang, Dr. D. Zhu, B. Shahid, Prof. R. Yang
CAS Key Laboratory of Bio-based Materials
Qingdao Institute of Bioenergy and Bioprocess Technology
Chinese Academy of Sciences, Qingdao 266101, China
E-mail: zhudq@qibebt.ac.cn; yangrq@qibebt.ac.cn
X. Yuan, B. Shahid
Center of Materials Science and Optoelectronics Engineering
University of Chinese Academy of Sciences, Beijing 100049, China
The ORCID identification number(s) for the author(s) of this article can be found under https://doi.org/10.1002/marc.201900035.

DOI: 10.1002/marc.201900035

 © 2019 WILEY-VCH Verlag GmbH & Co. KGaA, Weinheim

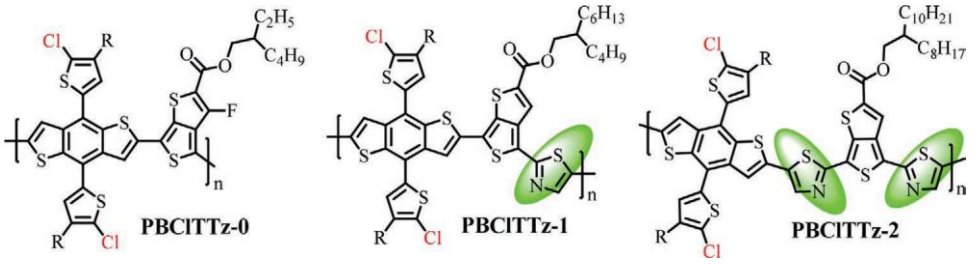

Figure 1. Molecular structures of the designed polymers.

devices with conventional structures, all polymers showed high V_{OC} of >0.94 V, reaching 1.01 V for PBClTTz-2-based solar cells, which is significantly higher than most TT-based polymers. Encouragingly, the solar cells based on polymer PBClTTz-1 with one thiazole unit exhibited the highest efficiency of 8.42% with a short-circuit current density (J_{SC}) of 14.09 mA cm^{-2} and a fill factor (FF) of 63.57%, which is superior to that of the fluorinated analogy PBClTTz-0 (6.85%). This result can be ascribed to the excellent surface morphology and weak recombination of the polymer:$PC_{71}BM$ blend film.

The synthetic route and the related characterization of the chlorinated BDT unit (M1) are presented in the Experimental Section (Supporting Information). Meanwhile, the quinoid monomers M2-M4 were prepared based on a previously reported method.[23–25] Three target polymers, PBClTTz-0, PBClTTz-1, and PBClTTz-2, were obtained via the Stille coupling reaction between monomer M1 and different TT acceptors, respectively, which were further purified via the Soxhlet extraction. The number-average molecular weight (*M*n) and polydispersity index (PDI) were measured via gel permeation chromatography (GPC) using 1,2,4-trichlorobenzene as an eluent at 150 °C. The polymers PBClTTz-0, PBClTTz-1, and PBClTTz-2 have *M*n of 81.6, 60.6, and 50.4 kDa with corresponding PDIs of 2.44, 2.44, and 2.38, respectively (Figure S1, Supporting Information). It is noteworthy that PBClTTz-0, with no thiazole unit, can dissolve well in common organic solvents at room temperature, such as chloroform (CF), chlorobenzene (CB), and *o*-dichlorobenzene (*o*-DCB). However, as the thiazole unit was introduced, the solubility of the polymer gradually decreased. Specifically, the polymer PBClTTz-2, having two thiazole units, only dissolved in hot CB or DCB, and the corresponding active layer thus should be spin-coated at 100 °C. In addition, from the thermogravimetric analysis, the decomposition temperatures (T_d) at 5% weight loss for the three polymers were 330, 375, and 348 °C for PBClTTz-0, PBClTTz-1, and PBClTTz-2, respectively (Figure S2, Supporting Information), indicating excellent thermal stability under an N_2 atmosphere.

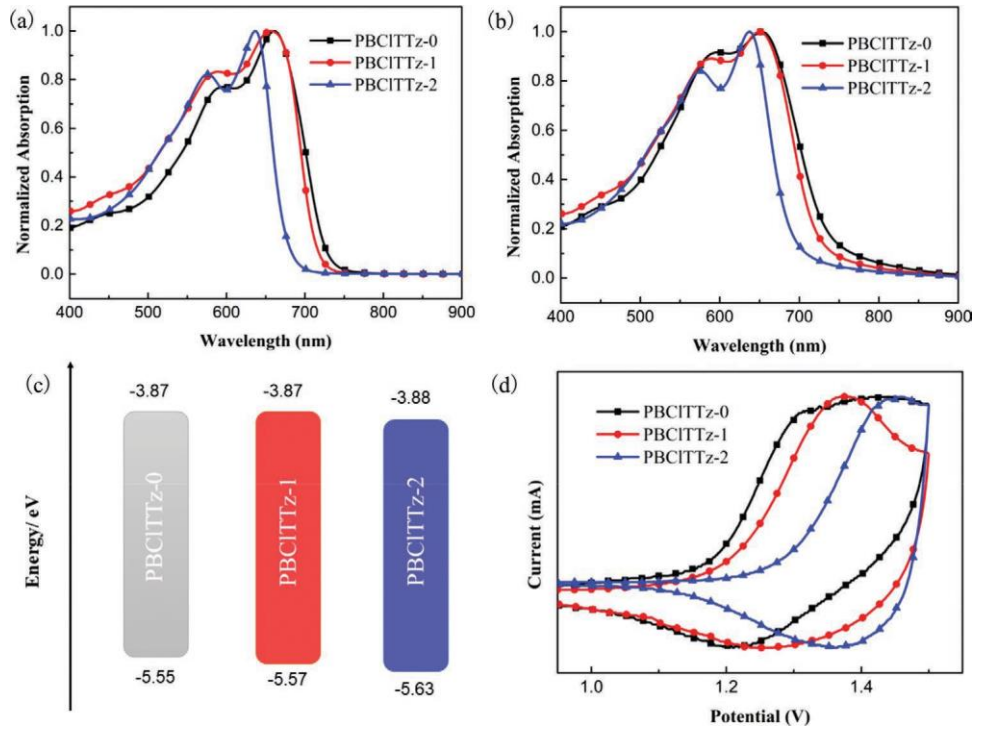

Figure 2. UV–vis absorption spectra of the polymers in solution (a), as film (b), energy level diagram of the polymers (c), and CV curves of the as casted film versus the SCE (d).

© 2019 WILEY-VCH Verlag GmbH & Co. KGaA, Weinheim

Table 1. The absorption properties and energy values of the polymers.

Polymer	Solution λ_{max} [nm]	Film λ_{max} [nm]	Film λ_{onset} [nm]	E_g^{opt} [eV][a)]	HOMO [eV]	LUMO [eV][b)]
PBClTTz-0	5 92 663	5 90 652	735	1.68	–5.55	–3.87
PBClTTz-1	5 91 658	5 91 650	729	1.70	–5.57	–3.87
PBClTTz-2	5 73 637	5 72 639	707	1.75	–5.63	–3.88

[a)]Estimated from the onset wavelength of the optical absorption: $E_g = 1240/\lambda_{onset}$; [b)]Calculated from the HOMO energy level and the optical bandgap.

The UV–vis absorption spectra of the as-synthesized polymers are shown in **Figure 2**a,b, and the corresponding optical parameters are summarized in **Table 1**. The polymers PBClTTz-0 and PBClTTz-1 exhibited similar absorption profiles with two main maximum peaks (λ_{max}) at approximately 590 and 655 nm. The absorption edges (λ_{onset}) were located at 735 and 729 nm, respectively corresponding to the optical band gaps of 1.68 and 1.70 eV. This phenomenon implied the same function for the Tz unit in the main backbone and the F atom on the side chain with regard to optical absorption. As another Tz unit was introduced, the optical absorption blueshifted further, which could be ascribed to the reduced ratio of the quinoid structure. In addition, compared to a nonchlorinated analogy, the polymers exhibited a hypsochromic shift of 30 to 40 nm, which is attributed to restrained intermolecular interactions caused by the larger atomic radius of chlorine atom.[23,25] Temperature-dependent UV–vis absorption spectroscopy was employed to investigate the aggregation behavior of the polymers in a dilute chlorobenzene solution (10^{-5} m) at temperatures ranging from room temperature to 100 °C (Figure S3, Supporting Information). As temperature increased, the defined shoulder peaks of all polymers gradually weakened, accompanied by several nanometers of blueshift, which implies that the intermolecular interactions decreased with continuous heating.

Cyclic voltammetry (CV) measurements were performed to study redox properties, and HOMO energy levels of the polymers were evaluated according to the empirical equation: $E_{HOMO} = -e(E_{ox} + 4.4)$ V (Figure 2d).[28] As listed in Table 1, the HOMO energy levels of PBClTTz-0, PBClTTz-1, and PBClTTz-2 are estimated to be −5.55, −5.57, and −5.63 eV, respectively. In detail, the introduction of a Cl atom significantly decreased the HOMO levels[23,25,29] due to the empty 3d orbitals on Cl that can accept delocalized π electrons.[30] Moreover, the similar HOMO energy levels for PBClTTz-0 and PBClTTz-1 support that the Tz unit in the main backbone also acted exactly the same as the F atom on the side chain. As the Tz units increased, the HOMO energy level decreased. The results verified that the Cl atom that was substituted on the side chain and the Tz unit that was incorporated into the main chain could significantly reduce the HOMO energy level, which could favor high V_{OC} in photovoltaic devices.[23,25,29]

To investigate the photovoltaic performance of the polymers, PSCs with the conventional device structure of ITO/PEDOT:PSS/polymer:$PC_{71}BM$/PFN/Al were fabricated, and various conditions (D/A weight ratios, solvent additive) were optimized (**Table 2**; Table S1, Supporting Information). The optimal current density–voltage (*J*–*V*) curves are presented in **Figure 3**a. Encouragingly, as expected, all of the polymers exhibited desirable V_{OC} of >0.94 V, which were 0.15–0.17 V higher than that of the corresponding nonchlorinated polymer, as well as one of the highest values obtained for TT-based polymers.[19,23,25,31] In the absence of a solvent additive, due to the unfavorable surface morphology of the active layer, the photovoltaic devices only showed poor efficiency of 2–5%. When the appropriate additive 1,8-diiodooctane (DIO) was added, all efficiencies greatly increased with improved J_{SC}. The polymer PBClTTz-1, with one thiazole unit, showed the same V_{OC} as PBClTTz-0, but with significantly increased J_{SC} and FF, as well as superior efficiency. The above result strongly confirmed that the thiazole-induced strategy could be more effective. However, when two thiazole units were incorporated into the backbone, the relatively low J_{SC} limited its photovoltaic performance, but with a greatly improved V_{OC} of 1.01 V due to unfavorable phase separation and serious recombination of the polymer:$PC_{71}BM$ blend film. Meanwhile, the V_{OC} trend was consistent with the trend of HOMO energy levels: as the Tz units increased, V_{OC} was further enhanced. Consequently, the device based on PBClTTz-1 showed the best efficiency of 8.42% with a V_{OC} of 0.94 V, J_{SC} of 14.09 mA cm^{-2}, and FF of 63.57%.

Furthermore, from the EQE curves under optimal conditions (Figure 3b), the photovoltaic devices based on polymer

Table 2. Photovoltaic parameters of the photovoltaic devices based on three polymers.

Polymer	DIO	V_{OC} [V]	J_{SC} [mA cm^{-2}]	FF [%]	PCE [%]	
					max	ave
PBClTTz-0	0	0.94	9.08	57.77	4.94	—
	3%	0.94	12.77	56.98	6.85	6.34
PBClTTz-1	0	0.93	7.85	57.53	4.20	—
	2%	0.94	14.09	63.57	8.42	8.02
PBClTTz-2	0	0.98	4.74	61.97	2.88	—
	3%	1.01	9.93	62.17	6.26	5.84

© 2019 WILEY-VCH Verlag GmbH & Co. KGaA, Weinheim

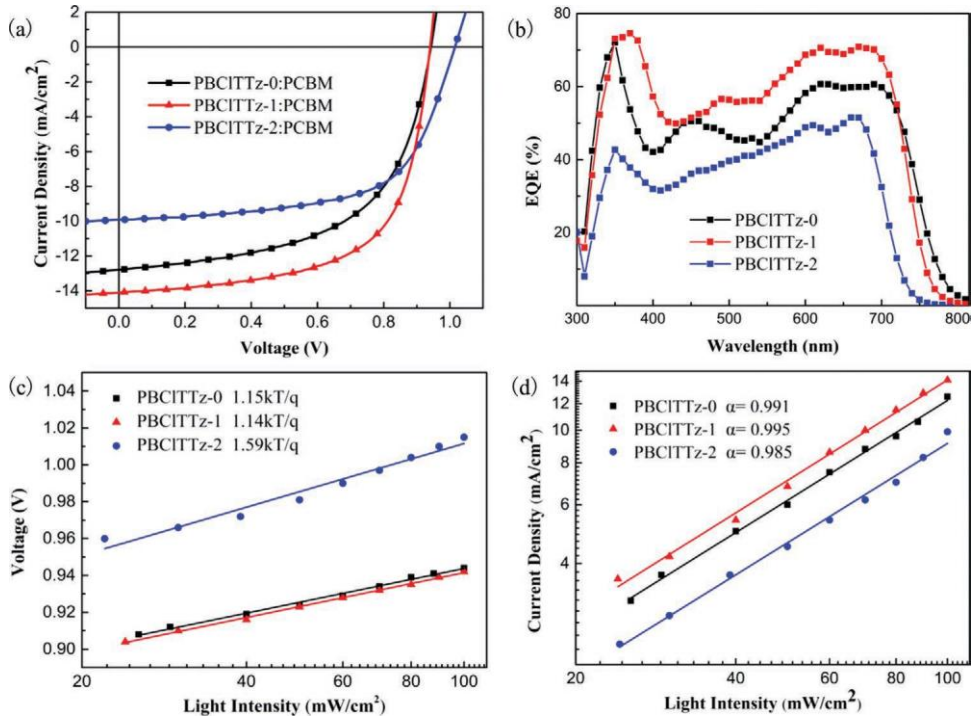

Figure 3. a) *J–V* curves under optimal conditions, b) EQE curves at the optimal conditions, c) V_{OC}, and d) J_{SC} versus light intensity (symbols) with linear fits to the data (solid lines) for the optimal devices based on polymers.

PBClTTz-1 exhibited clearly higher photo responses than those based on PBClTTz-0 and PBClTTz-2, ranging from 500 to 800 nm, leading to higher J_{SC}. In addition, the hole mobilities of the active layer were 8.58×10^{-5} cm^2 V^{-1} s^{-1} for PBClTTz-0, 9.45×10^{-5} cm^2 V^{-1} s^{-1} for PBClTTz-1, and 1.26×10^{-6} cm^2 V^{-1} s^{-1} for PBClTTz-2 (Figure S4, Supporting Information). High mobility could favor the effective transport of the charge carrier and reduced photocurrent loss in solar cells.[32,33] Thus, PBClTTz-1-based devices exhibited high J_{SC}, leading to excellent performance.The charge recombination characteristics in the active layers were investigated by the correlation of the V_{OC} and J_{SC} under different light intensity.

The charge recombination characteristics in the active layers were investigated by the correlation of V_{OC} and J_{SC} under different light intensities. The slope of V_{OC} versus ln(Plight) is close to nkT/q (k is Boltzmann's constant, T is temperature, and q is elementary charge), where n greater than 1 indicates trap-assisted recombination.[34,35] The slopes were 1.15, 1.14, and 1.59 kT q^{-1} for PBClTTz-0, PBClTTz-1, and PBClTTz-2-based devices, respectively (Figure 3c), indicating a reduced trap-assisted recombination for PBClTTz-1 devices. Furthermore, the correlation between J_{SC} and light intensity is according to the following formula: $J_{SC} \propto (P_{light})^{\alpha}$, where a fitting slope α is closer to 1 indicates weak bimolecular recombination.[36] As shown in Figure 3d, the extracted α value for PBClTTz-1-based devices is 0.995, higher than the other two (0.991 for PBClTTz-0, and 0.985 for PBClTTz-2). Consequently, PBClTTz-1-based devices could provide the best photovoltaic performance. In addition, to investigate the charge transfer behavior in the active layer, photoluminescence spectroscopic analysis (PL) was performed. For the polymers PBClTTz-0 and PBClTTz-1, it is apparent in Figure S5, Supporting Information, that the emission peaks of the pure film were almost completely quenched when blended with $PC_{71}BM$, suggesting the effective electron transfer from the polymer donor to the PCBM acceptor. However, the photoluminescence quenching efficiency of PBClTTz-2/$PC_{71}BM$ was only 68%, which is far below those of the other two polymers.

Transmission electron microscopy (TEM) measurements were performed to analyze the influence of a solvent additive on the surface morphology of the active layers. When without DIO, some polymers:$PC_{71}BM$ blend films exhibited obvious aggregations that are clear in **Figure 4**a–c. After the addition of DIO, the morphologies of PBClTTz-0 and PBClTTz-1-based blend films exhibited desirable phase separations with nanoscale domains and continuous interpenetrating networks, which favor efficient charge separation, leading to an increase in J_{SC}. Moreover, the desirable morphology can also benefit the effective diffusion of photogenerated exciton into the D/A interface, resulting in an improvement of FF.[37,38] Additionally, compared to that of the PBClTTz-0-based blend film, the PBClTTz-1/PCBM film exhibited more desirable fibril-like structures, which could be one main cause of the high J_{SC} associated with PBClTTz-1-based devices. In contrast, the poor phase separation for the PBClTTz-2/PCBM blend film could be the main reason for the low J_{SC}.

In summary, to obtain efficient solar cells with high V_{OC}, we designed and synthesized three new TT-based polymers, PBClTTz-0, PBClTTz-1, and PBClTTz-2, which were established systematically using an efficient chlorination strategy on the side chain and a thiazole-induced method in the

© 2019 WILEY-VCH Verlag GmbH & Co. KGaA, Weinheim

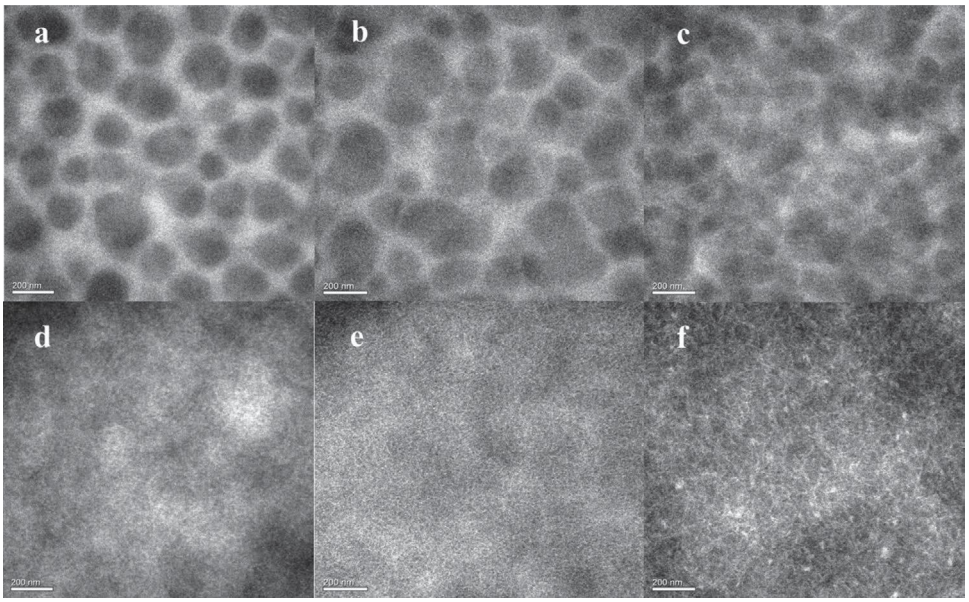

Figure 4. TEM images of polymer/$PC_{71}BM$ (1:1.5) blend films, PBClTTz-0 (a, without DIO, d, with 3% DIO), PBClTTz-1(b, without DIO, e, with 2% DIO), PBClTTz-2(c, without DIO, f, with 3% DIO).

polymer backbone. In addition, the influence of different thiazole numbers was also studied. As expected, all chlorinated polymers showed low HOMO energy levels of <−5.5 eV. When fabricated into the solar cells, all devices showed desirable V_{OC} of >0.94 V. Encouragingly, compared to the fluorinated analogy PBClTTz-0, the PBClTTz-1-based solar cells exhibited obviously enhanced J_{SC} of 14.09 mA cm^{-2} but with same V_{OC} of 0.94 V, demonstrating superior photovoltaic performance with an efficiency of 8.42%. This result is ascribed to restrained recombination, a more desirable fibril-like morphology, and higher hole mobility for PBClTTz-1-based devices. This work reveals the influence of the thiazole unit in a quinoid polymer backbone and confirms that the D-A(π)-Q strategy could be an efficient method to construct new light-harvesting polymers.

Supporting Information

Supporting Information is available from the Wiley Online Library or from the author.

Acknowledgements

The authors are deeply grateful to the National Natural Science Foundation of China (21604092, 51573205 and 51773220), the Shandong Provincial Natural Science Foundation (ZR2017ZB0314), DICP & QIBEBT (DICP&QIBEBT UN201709), and Dalian National Laboratory for Clean Energy (DNL) CAS for financial support.

Conflict of Interest

The authors declare no conflict of interest.

Keywords

backbone modification, chlorinated strategy, high open circuit voltage, polymer solar cells

Received: January 20, 2019
Revised: March 12, 2019
Published online: March 29, 2019

[1] G. Yu, J. Gao, J. C. Hummelen, F. Wudl, A. J. Heeger, *Science* **1995**, *270*, 1789.
[2] J. J. M. Halls, C. A. Walsh, N. C. Greenham, E. A. Marseglia, R. H. Friend, S. C. Moratti, A. B. Holmes, *Nature* **1995**, *376*, 498.
[3] L. Lu, T. Zheng, Q. Wu, A. M. Schneider, D. Zhao, L. Yu, *Chem. Rev.* **2015**, *115*, 12666.
[4] J. You, L. Dou, K. Yoshimura, T. Kato, K. Ohya, T. Moriarty, K. Emery, C. C. Chen, J. Gao, G. Li, Y. Yang, *Nat. Commun.* **2013**, *4*, 1446.
[5] J. Roncali, *Macromol. Rapid Commun.* **2007**, *28*, 1761.
[6] N. R. Armstrong, W. Wang, D. M. Alloway, D. Placencia, E. Ratcliff, M. Brumbach, *Macromol. Rapid Commun.* **2009**, *30*, 717.
[7] S. Zhang, Y. Qin, J. Zhu, J. Hou, *Adv. Mater.* **2018**, *30*, e1800868.
[8] S. Li, L. Ye, W. Zhao, H. Yan, B. Yang, D. Liu, W. Li, H. Ade, J. Hou, *J. Am. Chem. Soc.* **2018**, *140*, 7159.
[9] M. Zhang, X. Guo, S. Zhang, J. Hou, *Adv. Mater.* **2014**, *26*, 1118.
[10] H. J. Son, B. Carsten, I. H. Jung, L. Yu, *Energy Environ. Sci.* **2012**, *5*, 8158.
[11] C. Duan, J. J. v. Franeker, M. M. Wienk, R. A. J. Janssen, *Polym. Chem.* **2016**, *7*, 5730.
[12] Q. Peng, X. Liu, D. Su, G. Fu, J. Xu, L. Dai, *Adv. Mater.* **2011**, *23*, 4554.
[13] J. Min, Z.-G. Zhang, S. Zhang, Y. Li, *Chem. Mater.* **2012**, *24*, 3247.
[14] Y. Liang, Z. Xu, J. Xia, S. T. Tsai, Y. Wu, G. Li, C. Ray, L. Yu, *Adv. Mater.* **2010**, *22*, E135.
[15] Z. Wang, X. Xu, Z. Li, K. Feng, K. Li, Y. Li, Q. Peng, *Adv. Electron. Mater.* **2016**, *2*, 1600061.
[16] I. S. Kim, I. B. Kim, D. Y. Kim, S. H. Kwon, D. K. Ko, *Macromol. Rapid Commun.* **2016**, *37*, 1242.

 © 2019 WILEY-VCH Verlag GmbH & Co. KGaA, Weinheim

[17] H. J. Son, W. Wang, T. Xu, Y. Liang, Y. Wu, G. Li, L. Yu, *J. Am. Chem. Soc.* **2011**, *133*, 1885.
[18] J. H. Park, E. H. Jung, J. W. Jung, W. H. Jo, *Adv. Mater.* **2013**, *25*, 2583.
[19] H. Wang, P. Chao, H. Chen, Z. Mu, W. Chen, F. He, *ACS Energy Lett.* **2017**, *2*, 1971.
[20] S. Li, L. Ye, Q. Wang, S. Zhang, W. Zhao, J. Hou, *Org. Electron.* **2016**, *28*, 39.
[21] D. Zhu, L. Sun, Q. Liu, S. Wen, L. Han, X. Bao, R. Yang, *Macromol. Rapid Commun.* **2015**, *36*, 2065.
[22] D. Mo, H. Wang, H. Chen, S. Qu, P. Chao, Z. Yang, L. Tian, Y.-A. Su, Y. Gao, B. Yang, W. Chen, F. He, *Chem. Mater.* **2017**, *29*, 2819.
[23] D. Zhu, X. Bao, Q. Zhu, C. Gu, M. Qiu, S. Wen, J. Wang, B. Shahid, R. Yang, *Energy Environ. Sci.* **2017**, *10*, 614.
[24] D. Zhu, X. Bao, D. Ouyang, J. Wang, X. Yuan, Q. Wang, D. Zhou, S. Wen, R. Yang, *Nano Energy* **2017**, *40*, 495.
[25] D. Zhu, Q. Wang, Y. Wang, X. Bao, M. Qiu, B. Shahid, Y. Li, R. Yang, *Chem. Mater.* **2018**, *30*, 4639.
[26] D. Dang, W. Chen, S. Himmelberger, Q. Tao, A. Lundin, R. Yang, W. Zhu, A. Salleo, C. Müller, E. Wang, *Adv. Energy Mater.* **2014**, *4*, 1400680.
[27] Y. Yang, Z. G. Zhang, H. Bin, S. Chen, L. Gao, L. Xue, C. Yang, Y. Li, *J. Am. Chem. Soc.* **2016**, *138*, 15011.
[28] Y. Li, Y. Cao, J. Gao, D. Wang, G. Yu, A. J. Heeger, *Synth. Met.* **1999**, *99*, 243.
[29] S. H. Liao, H. J. Jhuo, Y. S. Cheng, S. A. Chen, *Adv. Mater.* **2013**, *25*, 4766.
[30] M. L. Tang, Z. Bao, *Chem. Mater.* **2011**, *23*, 446.
[31] S. Qu, H. Wang, D. Mo, P. Chao, Z. Yang, L. Li, L. Tian, W. Chen, F. He, *Macromolecules* **2017**, *50*, 4962.
[32] Q. Shi, H. Fan, Y. Liu, W. Hu, Y. Li, X. Zhan, *J. Phys. Chem. C* **2010**, *114*, 16843.
[33] Z. G. Zhang, J. Min, S. Zhang, J. Zhang, M. Zhang, Y. Li, *Chem. Commun.* **2011**, *47*, 9474.
[34] J. Li, Z. Liang, Y. Wang, H. Li, J. Tong, X. Bao, Y. Xia, *J. Mater. Chem. C* **2018**, *6*, 11015.
[35] A. K. Kyaw, D. H. Wang, V. Gupta, W. L. Leong, L. Ke, G. C. Bazan, A. J. Heeger, *ACS Nano* **2013**, *7*, 4569.
[36] H. Kim, B. Lim, H. Heo, G. Nam, H. Lee, J. Y. Lee, J. Lee, Y.Lee, *Chem. Mater.* **2017**, *29*, 4301.
[37] M. Drees, H. Hoppe, C. Winder, H. Neugebauer, N. S. Sariciftci, W. Schwinger, F. Schäffler, C. Topf, M. C. Scharber, Z. Zhu, R. Gaudiana, *J. Mater. Chem.* **2005**, *15*, 5158.
[38] J. Li, Y. Wang, Z. Liang, N. Wang, J. Tong, C. Yang, X. Bao, Y. Xia, *ACS Appl. Mater. Interfaces* **2019**, *11*, 7022.

 © 2019 WILEY-VCH Verlag GmbH & Co. KGaA, Weinheim